멤브레인(Membrane Journal)
Vol. 27 No. 4 August, 2017, 291-312

Print ISSN: 1226-0088
Online ISSN: 2288-7253
DOI: https://doi.org/10.14579/MEMBRANE_JOURNAL.2017.27.4.291

역삼투 공정을 위한 모델링 총설 및 새로운 복합적 막오염도의 제안

Albert S. Kim†

하와이대학교 토목환경공학과
(2017년 8월 28일 접수, 2017년 8월 29일 수정, 2017년 8월 29일 채택)

Review of Basics Reverse Osmosis Process Modeling: A New Combined Fouling Index Proposed

Albert S. Kim†

Civil and Environmental Engineering, University of Hawaii at Manoa, Honolulu, Hawaii 96822, USA
(Received August 28, 2017, Revised August 29, 2017, Accepted August 29, 2017)

요 약: 해수담수화는 최근 전 세계적으로 대두되고 있는 물부족 현상을 해결하기 위한 최적 기술 중 하나이다. 막분리 및 투과 현상의 근본적인 이해는 차후의 막여과 기술의 발전을 위해서 뿐만 아니라, 현재 막기술 증진을 위한 통합적 디자인, 최적화 제어법, 그리고 중장기적 유지관리를 위해서도 매우 중요하다. 이에, 본 연구는 물질 전달 및 여과 현상에 대한 기존의 주요 모델들을 상세히 재검토하고, 통계물리학에 근간하여 주요 막분리 현상들을 이론적으로 분석하며, 원천적 모델에 기초한 물리적 의미와 그들이 실제 막공정에서 미치는 영향들에 대해서 함축적으로 토의하고자 한다. 이론적 재검토의 과정에서 새로이 유도된 복합적 막오염도(Combined Fouling Index (CFI))의 소개도 포함한다.

Abstract: Seawater desalination is currently considered to be one of the primary technologies to resolve the global water scarcity problem. A basic understanding of membrane filtration phenomena is significant not only for further technological development but also for integrated design, optimal control, and long-term maintenance. In this vein, the present work reviews the major transport and filtration models, specifically related to reverse osmosis phenomena, provides theoretical insights based on statistical mechanics, and discusses model-based physical meanings as related to their practical implications.

Keywords: *Reverse Osmosis, Concentration Polarization, Solution-Diffusion, Model, Combined Fouling Index (CFI), Modified Fouling Index (MF), Membrane Process Modeling*

1. Introduction

The first commercial reverse osmosis (RO) membrane was developed by two researchers, S. Loeb and S. Sourirajan in early 1960 at University of California, Los Angeles (UCLA). After the pioneering work, RO technology has been rapidly developed and widely applied in a variety of separation and filtration fields, especially for seawater desalination. Fig. 1(a) shows original photo images of the prototype desalination cell using fabricated cellulose acetate membranes[1]. Their project entitled “Sea Water Demineralization by Means of Semipermeable Membrane” was carried out under the sponsorship of the Statewide Water Resources Center program in Sea Water Conservation Research. S. Loeb and S. Sourirajan were listed as project leaders, and the other four personnel include L. Graham, A. Noeggerath, R. Sayano, and M. Accomazzo. The report was signed by Prof. J. M. English, vice-chairman of research, in the *Department of Engineering*, UCLA. Fig. 1(b) shows the “life test assembly” which contains the desalination cell and circulating and pressurizing pumps. The life test indicates the filtration experiment, which operated 24 hours per day for two

†Corresponding author(e-mail: albertsk@hawaii.edu, http://orcid.org/0000-0002-9027-4616)

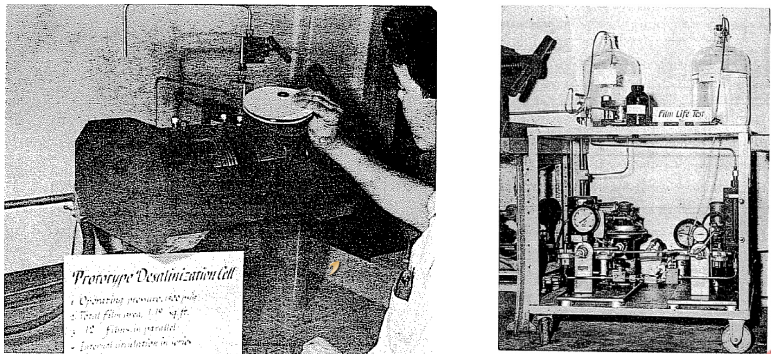

(a) (b)

Fig. 1. (a) Assembling film packages in prototype desalination cell and (b) life test assembly (Fig. 3 and 8 of Ref.[1], respectively. Reprinted).

months. The feed solution was 5.25 percent of seawater (generated within the system), and the applied pressure was 1500 psi (= 103.4 bar). During the first seven days (period 1) from the fall of 1959, water flux and permeate concentration were measured as 6.4 gal/ft^{2}day (= 10.87 liter/m^2 h, LMH) and 0.042 percent, respectively. From the second to the fourth week (period 2), water flux decreased from 6.4 to 5.2~5.6 gal/ft^{2}day and the permeate concentration remained as 0.040 $\pm$ 0.003 percent. In period 1 and 2, the rejection ratios were calculated as 99.20 and 99.24 percent, respectively. In period 3 of four weeks, the average flux was measured as 4.75 gal/ft^{2}day with 98.97 percent of rejection. Finally, the total cost was estimated as \$0.60 per 1,000 gallons, i.e., \$0.16/m^3, which is cheaper than the present water production rate by Sorek plant, in Israel, that currently produces 624,000 m^3/day (26,000 m^3/hour)[2]. In the 1960 report, Loeb and Sourirajan's future work includes standardization of film-fabricating techniques, fabrication cost estimation, and investigation of separation mechanisms, which have been vigorously conducted by subsequent researchers till date. The fabricated membrane is later explicitly called Loeb-Sourirajan membrane, and the more detailed stories can be found elsewhere[3,4].

Various mechanisms and models were suggested to explain the RO phenomena. The sieving mechanism [5] indicates that the separation occurs due to the difference between molecular sizes of solvent and solutes. The wetted-surface mechanism[6,7] treats the membrane as very wettable material so that water tends to cling to the membrane surface. The solution-diffusion model[8,9] followed by the solution-diffusion-imperfection model[10] assumes that both solvent and solutes *dissolve* in the homogeneous nonporous surface layer of the membrane and then *diffuse* without significant solvent-solute interactions. The preferential sorption & capillary flow mechanism[5,11,12] proposes a critical pore size, twice (or smaller than) the water layer thickness on the membrane surface, to allow only solvent transport through the membrane. Among these models for RO processes, the solution-diffusion model was most widely accepted for explanation and prediction of RO processes. Transport of solvent and solutes was universally explained using the trans-membrane chemical potential[13], in which transition from the solution-diffusion to the pore flow was also investigated. Later, the solution-diffusion model was reformulated as a pressure-driven diffusion process using rigorous thermodynamic boundary conditions, which led to nonlinear responses at high pressure[14]. Specifically, the coupling between solvent and solutes was considered using the Maxwell-Stefan formulation for multi-component diffusion[14].

Although the models as mentioned earlier were used to fundamentally explain the RO phenomena, they mostly dealt with specific mass transport mechanisms across the polymer membrane, of which thermody-

namic state is assumed to be quite close to the (pure) static equilibrium. To the best of my knowledge, non-equilibrium thermodynamics is still at a nascent stage in theoretical statistical physics. The front-end improvement is a theory to investigate the thermo-electric phenomena, such as transference phenomena in electrolytes and heat conduction in an anisotropic medium, viewed as coupled, irreversible processes[15,16]. A thermodynamic system was relaxed from the pure equilibrium to one where the microscopic reversibility could be assumed. This means that an irreversible system of non-equilibrium can be viewed as a collection of a number of small local subregions, having individual processes, in which the time-reversal is guaranteed. The time-reversal indicates that an evolving system from its initial condition returns to the original state if time t is reversed to $-t$. In other words, an average rate of an individual process is equal to the average rate of its reverse process. In his work, Onsager described the *irreversible* process using the entropy change rate. A phenomenological driving force was defined as a partial derivative of the entropy with respect to specific fluxes (of multi-species or heat).

The first irreversible transport (IRT) model was developed to explain the transfer of non-electrolytes through membranes using Onsager's reciprocal theorem by Kedem and Katchalsky[17], followed by Spiegler and Kedem[18]. These irreversible transport models require empirically determining a few model parameters, which is a practical trade-off to use more realistic models. Most membrane systems are thermodynamically open to the ambient environment. If one of the systems is in a thermodynamic state that is quite close to a static equilibrium, then the irreversible model parameters often converge to those of limiting values of the pure equilibrium. In this case, irreversible thermodynamic filtration models become mathematically identical to the solution-diffusion model for RO in terms of functional interdependences between the solvent and solute fluxes and their relationship with the effective driving force.

More rigorous theoretical investigation of RO processes using the non-equilibrium thermodynamics or simply steady-state thermodynamics is necessary to develop next-generation membrane technology. Currently, there are a number of excellent articles that provide well-summarized technical information and future perspectives of RO technology[19-27]. Fundamental studies and reviews on the future membrane technologies in various aspects can be found elsewhere[28-32]. Continuing in this vein, the current work will deal with in-depth and detailed analysis of the solution-diffusion model in various aspects as applied to process simulations with a limited literature review and will additionally provide theoretical derivations for the fouling phenomena on the RO membrane. This paper aims to give a clear picture of the RO membrane as a platform of coupled thermo- and fluid dynamic phenomena and contribute to a solid curriculum for membrane engineering.

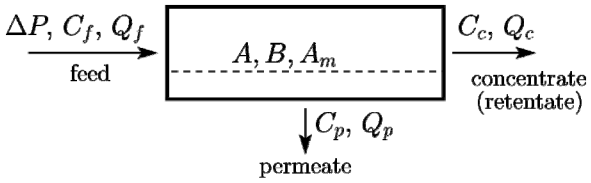

Fig. 2. A schematic of the RO process.

2. Theory and Simulation Review

2.1. Basic RO process modeling

2.1.1. Mass balance equations

Fig. 2 shows the RO schematic, consisting of ten thermodynamic and fluid dynamic variables. Hydraulic pressure ΔP is applied to the feed stream of concentration C_f and results in feed flow rate Q_f. A portion of the feed stream passes through the RO membrane characterized by solvent permeability A, solute permeability B, and surface area A_m. This product stream is called permeate stream having concentration C_p (usually much lower than C_f) and outflow rate Q_p. The concentrate (often called retentate) stream has concentration C_c (higher than C_f due to the solvent permeation) flowing with its outflow rate Q_c. The study objective of this basic RO modeling is to calculate output concen-

trations and flow rates in terms of input and operating conditions. To do that, we define two representative parameters used to evaluate the performance of RO membranes: rejection ratio (which we will later call *observed* rejection)

$$R = 1 - \frac{C_p}{C_f} \tag{1}$$

and recovery ratio

$$Y = \frac{Q_p}{Q_f} \tag{2}$$

which express the quality and quantity of the solvent product, respectively.

For both solvent and solute mass transport, the input rate is equal to a sum of two output rates:

$$Q_f = Q_p + Q_c \tag{3}$$

$$C_f Q_f = C_p Q_p + C_c Q_c \tag{4}$$

Solvent flux [m/sec], i.e., the collected volume of water transported through the membrane per unit time per unit membrane surface area, is described as

$$J_w = \frac{Q_p}{A_m} = A(\Delta P - \Delta\pi) \tag{5}$$

where $\Delta\pi = \pi_f - \pi_p$ is the osmotic pressure difference between the feed (π_f) and the permeate (π_p) streams. Solute flux, i.e., the solvent flux multiplied by permeate concentration (mg/l · m/sec) is expressed as

$$J_s = B\left(C_f - C_p\right) \tag{6}$$

$$= C_p J_w \tag{7}$$

Substituting Eq. (2) in (4) allows us to express the retentate concentration using feed and permeate concentrations and recovery ratio:

$$C_c = \frac{C_f - C_p Y}{1 - Y} \tag{8}$$

The permeate concentration of Eq. (7) is rewritten as

$$C_p = \frac{J_s}{J_w} = \frac{C_f}{1 + \frac{A}{B}(\Delta P - \Delta\pi)} \tag{9}$$

and flow rates of the permeate and retentate streams are then represented using Q_f and Y:

$$Q_p = Q_f Y \tag{10}$$

$$Q_c = Q_f(1 - Y) \tag{11}$$

Note that we initially had total ten variables (shown in Fig. (2)), of which subset consists of six knowns: $\{\Delta P, A, B, A_m, C_f, Q_f\}$. The four balance Egs. (3)-(7) of solvent and solute transfer rates make the RO process modeling mathematically solvable.

2.1.2. Analytic solutions with van't Hoff-type osmotic pressure

If the osmotic pressure is linearly proportional to the solute concentration, then its transmembrane difference is

$$\Delta\pi = b\left(C_f - C_p\right) \tag{12}$$

where b is a proportionality. In van't Hoff's equation, we have $b = \mathcal{R}T$, where $\mathcal{R}$ is the gas constant and T is the absolute temperature of the membrane system. (J. H. van't Hoff was recognized by the Nobel Prize committee for his discovery of "the laws of chemical dynamics and osmotic pressure in solutions" and received the first Nobel Prize in Chemistry in 1901.) Substitution of (12) into (9) gives

$$C_p = C_\alpha\left[\sqrt{1 + C_\beta^2 / C_\alpha^2} - 1\right] \tag{13}$$

where

$$C_\alpha = \frac{BA^{-1} + \Delta P - bC_f}{2b} \tag{14}$$

and

$$C_\beta = \sqrt{\frac{BC_f}{Ab}} \tag{15}$$

Note that C_α and C_β have a unit of solute concentration. For simplicity, let's set $\psi = C_\beta/C_\alpha$. If $\psi \ll 1$, then one can approximate the terms in the parenthesis of Eq. (13) using the Taylor expansion as

$$\sqrt{1+\psi^2} - 1 = \left[1 + \frac{1}{2}\psi^2 + \cdots + O(\psi^4)\right] - 1 \approx \frac{1}{2}\psi^2 = \frac{1}{2}\left(\frac{C_\beta}{C_\alpha}\right)^2 \tag{16}$$

where $O(\psi^4)$ indicates the remaining terms of ψ^4 and higher, and simplify the functional form of C_p as

$$C_p \approx \frac{C_\beta^2}{2C_\alpha} = \frac{C_f}{1 + \frac{A}{B}(\Delta P - \pi_f)} \tag{17}$$

which is equivalent to Eq. (9) with a condition of $C_p \ll C_f$, and hence indicating $\Delta\pi \approx \pi_f$. However, note that Eq. (9) is an implicit solution for C_p, because $\Delta\pi$ includes C_p itself. For an accurate calculation, C_p of Eq. (17) needs to be used to calculate $\Delta\pi$ in Eq. (12), and an iterative method should continue until C_p in Eq. (9) converges to a specific constant value. The accurate calculation of C_p is important not only for RO but also for NF, in which C_p is comparable with C_f. In this case, higher-order terms in Eq. (16) must be important for such low-rejection filtration processes, in which the widely-used approximation of $C_p \ll C_f$ (in RO) is questionable. As the exact solution of Eq. (13) has a perfect closure form, calculations of C_c, Q_p (or J_w), and Q_c are straightforward using C_p of Eq. (13) without any approximation or numerical iterations.

2.1.3. Causes and effects

Fig. 3 shows how output variables C_p, Q_p and C_c change with respect to input variables of ΔP, Q_f and C_f, while A, B and A_m are assumed to be invariant during operations. Calculation of Q_c is straightforward using the solvent mass balance of Eg. (11). While one of the three input variables changes with the other two remaining fixed, variations of output variables with respect to the solely changing input variable are analyzed as follows using Eqs. (8)-(10). Fundamental aspects of the solution-diffusion model will be discussed in the later sections.

2.1.3.1. Effect of pressure ΔP

First, we let C_f and Q_f remain constant and increase only applied pressure ΔP. This type of analysis is mathematically equivalent to calculating partial derivatives of C_p, Q_p and C_c with respect to ΔP.

(a) In most RO cases of a high rejection ratio (close to 1.0), $B \ll J_w$ must be a good approximation (Note that B and J_w have the same unit of velocity [m/s]). As J_w is proportional to ΔP, the permeate concentration C_p of Eq. (9) decreases with ΔP:

$$\frac{C_p}{C_f} = \frac{1}{1 + J_w/B} \approx \frac{B/A}{(\Delta P - \Delta\pi)} \tag{18}$$

If concentration polarization (CP) is negligible above the membrane surface, one can approximate $\Delta\pi \approx \pi_f$, $C_p \ll C_f$, and hence $C_p \propto 1/\Delta P$. One may apply a higher pressure to decrease the permeate concentration C_p, to be obtained by increasing permeate flux J_w. If the feed concentration is close to the seawater concentration having the osmotic pressure about 400-500 psi, then a decrease in C_p with respect to ΔP is not as much as that of brackish water of a few thousand mg/l. As one increases ΔP, the enhanced pressure

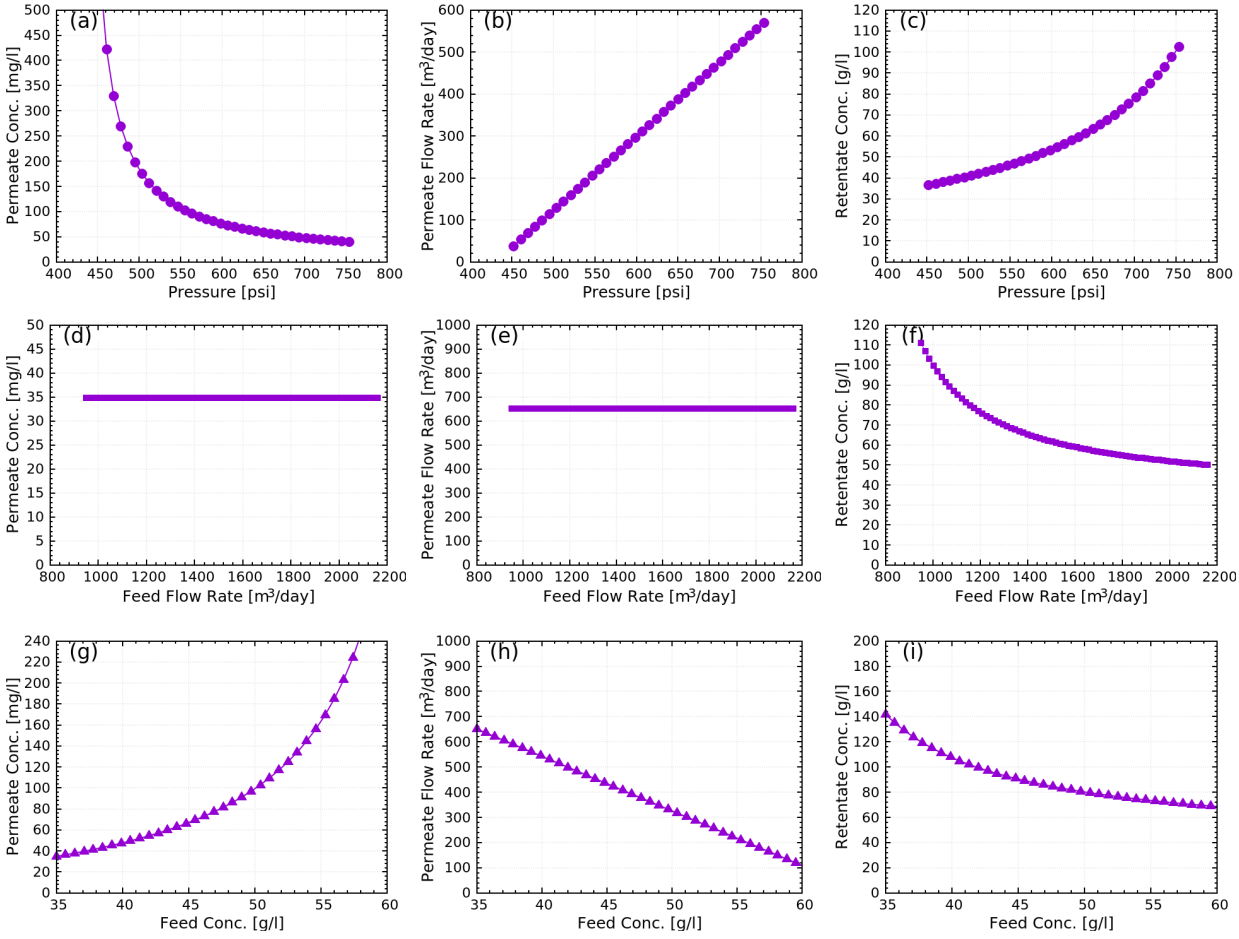

Fig. 3. Theoretical causes and effects in basic RO modeling. Parameters used are $T = 25$°C, $A_m = 150\,\mathrm{m}^2$, $A = 1.36 \times 10^{-7}$ m/s psi, $B = 5.0 \times 10^{-8}$ m/s, $Q_f = 864$ m³/day, $C_f = 35\,C_f = 35$ g/l, $\Delta P = 800$ psi. Three variables of ΔP, Q_f and C_f are selected as independent variable in the first, second and third rows, respectively. Variations of C_p, Q_p and C_c are calculated with respect to one independent variable while the rest two are kept constant.

pushes more water to the membrane to have a higher permeate flux, J_w. In this case, the convective solute transport (roughly equal to $C_f J_w$) increases at the membrane surface. As the membrane rejects solute ions, C_m on the membrane surface increases from C_f, providing a higher osmotic pressure difference between the feed side and the permeate side of membrane surface, i.e., $\Delta\pi_m\left(=\pi_m-\pi_p\right) > \Delta\pi_f\left(=\pi_f-\pi_p\right)$. The increase in $\Delta\pi_m$ is a partial feedback from increased ΔP, so that a decrease in C_p is lessened by the CP phenomena, which is fundamentally inevitable (See section 2.2 for details).

(b) The permeate flow rate is conceptually equivalent to the permeate flux, because the available membrane surface area A_m is usually fixed. (See Eq. (5).) This indicates that the variation of Q_p with respect to ΔP is the same as that of J_w. Here, we assume for simplicity that $\Delta\pi$ is insensitive to ΔP, and J_w is not meaningful if $\Delta P \leq \Delta\pi$. As indicated in Fig. 3(b), the onset of non-zero Q_p occurs when ΔP exceeds $\Delta\pi$. After that, Q_p monotonously increases with ΔP and the slope is equal to $A \cdot A_m$ from Eq. (5). In reality, measured Q_p resides below the linear line, because the CP increases the osmotic pressure difference and therefore decreases the effective pressure, $\Delta P_{\mathrm{eff}} = \Delta P - \Delta\pi_m$.

(c) As C_p decreases with respect to ΔP, more solutes are rejected by the membrane. Overall, the amount

of solutes retained per unit fluid volume, i.e., retentate concentration C_c, increases with ΔP. For high rejection of $C_p \ll C_f$, we can neglect $C_pY = C_f(1-R)Y$ in the numerator of Eq. (8) to have:

$$C_c \approx \frac{C_f}{1-Y} \tag{19}$$

Note that Y is proportional to $Q_p \propto J_w \propto \Delta P_{\text{eff}}$. C_c is therefore linearly proportional to ΔP if and only if the recovery ratio is small (i.e., $Y \ll 1$). To validate this, one can use Taylor's series of C_c with respect to Y:

$$C_c = C_f\left(1 + Y + O(Y^2)\right) \tag{20}$$

Otherwise, the higher-order terms become significant and C_c must non-linearly increase with ΔP, as shown in Fig. 3(c).

2.1.3.2. Effect of feed flow rate Q_f

(d) The feed flow rate Q_f usually does not significantly change the characteristics of the permeate stream, unless ΔP depends on Q_f or vice versa. The permeate concentration is pseudo-independent of Q_f.

(e) In the same vein, the permeate flow rate is indifferent to the feed flow rate because Q_p primarily depends on the applied pressure ΔP. The amount of water that passes in the longitudinal direction (tangential to the membrane surface) in the feed stream does not noticeably change the permeate flux J_w or permeate flow rate Q_p.

(f) Because $Q_f = Q_p + Q_c$, for a constant Q_p, Q_c increases with Q_f. Eq. (19) can be then rewritten as

$$C_c = C_f\frac{Q_f}{Q_c} = C_f\left(1 + \frac{Q_p}{Q_f - Q_p}\right) \tag{21}$$

to show that C_c gradually decreases with Q_c or Q_f.

2.1.3.3. Effect of feed concentration C_f

(g) When the applied pressure is much higher than the feed osmotic pressure, C_p is small and linearly proportional to C_f; in other words, $C_p/C_f \ll 1$. When the applied pressure is comparable with the osmotic pressure, C_p versus C_f curve shows a non-linearly increasing trend, which is above the linear line. Eq. (9) indicates that the increase in C_f secondarily contributes to $\Delta\pi_m$ by increasing C_m, and finally reduces ΔP_{eff} and J_w. As a consequence, the solvent and solute fluxes decrease and increase, respectively, with C_f, and therefore the permeate concentration C_p increases.

(h) When ΔP and Q_f are fixed, Q_p linearly decreases with respect to C_f and hence C_m:

$$Q_p = A_m J_w \propto \Delta P - \Delta\pi_m = \Delta P + bC_p - bC_m \tag{22}$$

The permeate flow rate vanishes when $\pi_m = \Delta P + \pi_p \approx \Delta P$.

(i) When recovery is small, i.e., $Y \ll 1$ or $Q_p \ll Q_f$, the retentate concentration C_c does not change significantly from the feed concentration level, i.e., $C_c \sim C_f$. As C_f increases when ΔP is finitely higher than π_f, Y decreases because Q_p monotonously decreases with C_f. Therefore, the slope of C_c versus C_f plotted from Eq. (8) also decrease with C_f: $1/(1-Y) \approx 1 + Y + Y^2 + Y^3 + \cdots$. Note that $(1-Y)^{-1} > 1$ indicates C_c is unconditionally higher than C_f, except for the zero-recovery case. The slope of Fig. 3(i) can be calculated as

$$\frac{\partial C_c}{\partial C_f} = \frac{1 - Y_0}{\left[1 - Y_0 + Y_1 C_f\right]^2} \tag{23}$$

where $Y_0 = A_m A\Delta P/Q_f$ and $Y_1 = A_m Ab/Q_f$. Parameter values in Fig. 3 gives the Y_0 higher than 1.0, which provides a negative value of $\partial C_c/\partial C_f$. Therefore, Fig. 3(i) shows the gradually decreasing behavior of C_c with respect to C_f.

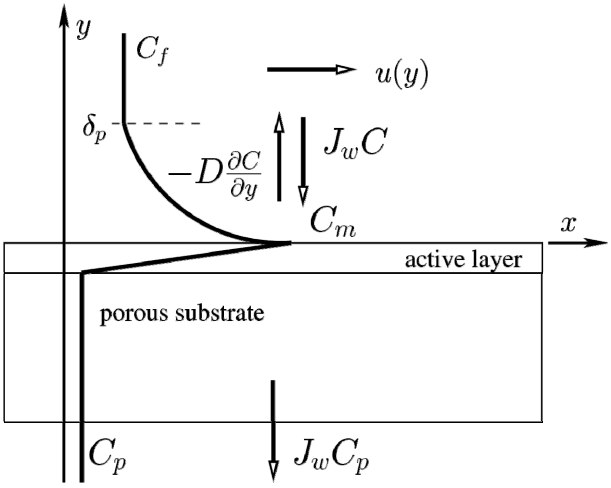

Fig. 4. Schematic of concentration profile across the membrane in the crossflow.

2.2. Concentration Polarization

2.2.1. Phenomena

Fig. 4 shows a schematic of diffusive and convective transport of solutes near the membrane surface. During the RO/NF filtration process, pressurized feed stream of concentration C_f flows in a tangential (x-) direction to the membrane with velocity u. Solutes are rejected by the membrane, whereas solvent (water) molecules pass through it. The permeate concentration C_p is therefore much lower than the feed concentration C_f in proper operations. The hydraulic pressure gradient between the bulk and permeate stream generates the solvent flow across the membrane, which is defined as the permeate flux J_w, i.e., the volume of solvent passing through the membrane per unit membrane surface area: a unit of J_w is [m^3/m^2 s], equivalent to [m/s] or [μm/s]. As the transverse solvent flow brings solutes down to the membrane surface, solutes are retained on the membrane surface where concentration C_m is higher than C_f. This phenomenon of the uneven or biased concentration distribution near the membrane surface is called the concentration polarization (CP), and the region where the CP occurs is called the CP layer. δ_p denotes the thickness of the CP layer above which the concentration remains C_f.

2.2.2. Mass balance

Solutes are transported from the bulk phase toward the membrane by two mass transfer mechanisms, i.e., convection and diffusion, which are balanced as

$$J_w C - \left(-D\frac{\partial C}{\partial y}\right) = J_w C_p \tag{24}$$

Here, $J_w C$ is the convective transport of solutes from the bulk phase toward the membrane. Within the concentration polarization layer, $0 < y < \delta_p$, the solute concentration $C(y)$ decreases with respect to y so that $-D\partial c/\partial y$ is positive and indicates the magnitude of diffusive transport of solutes from the membrane surface back to the bulk phase. Therefore, specific boundary conditions are:

$$C(y = 0) = C_m \tag{25}$$

$$C(y = \delta_p) = C_f \tag{26}$$

The CP layer of thickness δ_p is usually much smaller than the channel height of the feed flow. Within the CP layer, it is appropriate to approximate that the permeate flux J_w is constant with respect to y and the concentration is independent of the axial position x of the membrane surface. Then, the partial derivative of $\partial C/\partial y$ in Eq. (24) becomes its ordinary differential, i.e., $\mathrm{d}C/\mathrm{d}y$. Integration of Eq. (24) with respect to y using boundary conditions of Eqs. (25) and (26) yields

$$\frac{C_m - C_p}{C_f - C_p} = e^{J_w/k_f} \tag{27}$$

where $k_f = D/\delta_p$ is the mass transfer coefficient, indicating how quickly solutes back-diffuse from the membrane to the bulk phase. (See section A.1 for the detailed derivation of Eq. (27).) Usually, δ_p (or k_f) is unknown and often estimated using empirical correlations (originally developed to describe heat transfer phe-

nomena), because a coupled mass-transfer equation using transversely varying crossflow velocity is hard to solve. The right-hand side of Eq. (27) is interpreted as the ratio of excessive concentrations at the membrane surface to that of the bulk phase. In RO/NF, this ratio is roughly between 1 and 3.

2.2.3. Rejection ratios

From Eq. (27), the solute concentration on the membrane surface is rewritten as

$$C_m = C_p + \left(C_f - C_p\right) e^{J_w/k_f} \tag{28}$$

$$= C_p + C_f R_{\text{obs}}\, e^{J_w/k_f} \tag{29}$$

where R_{obs} is the *observed* rejection ratio, defined as

$$R_{\text{obs}} = 1 - \frac{C_p}{C_f} \tag{30}$$

which indicates the fraction of solutes retained by the membrane. The permeate concentration can be calculated using R_{obs}:

$$C_p = C_f\left(1 - R_{\text{obs}}\right) \tag{31}$$

and now we can eliminate C_p in Eq. (29) to derive

$$\frac{C_m}{C_f} = 1 + R_{\text{obs}}\left(e^{J_w/k_f} - 1\right) \tag{32}$$

For the perfect rejection ($R_{\text{obs}} = 1.0$), C_m reduces to

$$C_m = C_f\, e^{J_w/k_f} \tag{33}$$

as a product of C_f and the exponential factor. In addition to R_{obs}, the *intrinsic* rejection is defined as

$$R_{\text{int}} = 1 - \frac{C_p}{C_m} \left(> R_{\text{obs}}\right) \tag{34}$$

Substitution of Eq. (28) in (34) derives

$$\frac{C_m}{C_f} = \frac{e^{J_w/k_f}}{R_{\text{int}} + (1 - R_{\text{int}})e^{J_w/k_f}} > 1.0 \tag{35}$$

which requires known values of J_w, k_f, and R_{int}. In normal RO processes, measured J_w is about a few $\mu\text{m/s}$, k_f can be estimated using empirical correlations, and R_{int} is often close to 1.0. If the intrinsic rejection R_{int} is close to zero, the right-hand side converges to one. No concentration polarization occurs and the concentration has an even distribution along the y-direction, i.e, $C_m \simeq C_f$. Similarly, if the membrane resistance is very high (e.g., almost impermeable when deleteriously fouled), the solvent flux becomes very small, i.e., $J_w \to 0$. Hence, we calculate that:

$$e^{J_w/k_f} \approx 1 + O\left(\frac{J_w}{k_f}\right) \approx 1.0 \tag{36}$$

or equivalently $C_m \simeq C_f$.

2.3. Solution-diffusion model

2.3.1. Governing equations based on Fick's law

2.3.1.1. Solvent Transport

We assume that water transport through the normal membranes is by diffusion through a single membrane phase and so write transport equation of water:

$$J_w = -D_w \nabla C_w \tag{37}$$

where C_w and D_w are concentration and diffusivity of water *dissolved* in the membrane[33]. We accept the *Henrian* approximation that in an isothermal environment

$$\mu_w = RT \ln\, C_w + \mu_{\text{wo}} \tag{38}$$

where μ_w is the chemical potential of the water and μ_{wo} is an isothermal constant independent of C_w. Substitution of Eq. (38) in (37) gives

$$J_w = \frac{D_w C_w}{RT} \nabla \mu_w \approx \frac{D_w C_w}{RT} \frac{\Delta \mu_w}{\delta_m} \tag{39}$$

which represents the solvent flux driven by the chemical potential gradient $\nabla \mu_w \simeq \Delta \mu_w / \delta_m$, where $\Delta \mu_w$ is the chemical potential difference across the membrane of thickness δ_m. In pressure-driven membrane separation processes, the chemical potential of water may be governed by the applied pressure and water concentration and then it can be expanded as

$$\mathrm{d}\mu_w = \left(\frac{\partial \mu_w}{\partial C_w}\right)_{P,T} \mathrm{d}C_w + \left(\frac{\partial \mu_w}{\partial P}\right)_{C_w,T} \mathrm{d}P \tag{40}$$

Integration of Eq. (40) across the membrane gives

$$\begin{aligned} \Delta \mu_w &= \int \left(\frac{\partial \mu_w}{\partial C_w}\right)_{P,T} \mathrm{d}C_w + \int \left(\frac{\partial \mu_w}{\partial P}\right)_{C_w,T} \mathrm{d}P \\ &= \int \left(\frac{\partial \mu_w}{\partial C_w}\right)_{P,T} \mathrm{d}C_w + \bar{v}_w \Delta P \end{aligned} \tag{41}$$

If the applied pressure is equal to the osmotic pressure difference $(\Delta P = \Delta \pi)$, then mass fluxes are zero since the chemical potential has zero gradient. Hence, we obtain

$$\int \left(\frac{\partial \mu_w}{\partial C_w}\right)_{P,T} \mathrm{d}C_w = -\bar{v}_w \Delta \pi \tag{42}$$

and therefore

$$\Delta \mu_w = \bar{v}_w (\Delta P - \Delta \pi) \tag{43}$$

where $\bar{v}_w$ is the molar volume of the solvent. Substitution of Eq. (43) in (39) gives the solvent flux:

$$J_w = \frac{D_w C_w \bar{v}_w}{RT \delta_m} (\Delta P - \Delta \pi) = A(\Delta P - \Delta \pi) \tag{44}$$

where

$$A = \frac{D_w C_w \bar{v}_w}{RT \delta_m} \tag{45}$$

is called the solvent permeability having a unit of $[m/s \cdot atm]$, which is often assumed to be independent of ΔP. Eq. (44) indicates that the water flux through the membrane is proportional to the effective pressure, i.e. the difference between ΔP and $\Delta \pi$. The origin of this conclusion is from the thermodynamic relationship:

$$\left(\frac{\partial \mu_w}{\partial P}\right)_{C_w,T} = \bar{v}_w \tag{46}$$

or equivalently

$$\mu_w = \bar{v}_w \Delta P + f(C_w, T) \tag{47}$$

where f is an arbitrary function of C_w and T. Comparison of Eqs. (47) and (40) gives a self-consistent result in terms of specific dependence of μ_w on ΔP, C_w, and T.

2.3.1.3. Solute Transport

The transmembrane solute diffusion is also assumed to be Fickian:

$$J_s = -D_s \nabla C_s \approx \frac{D_s}{\delta_m} \Delta C_s = B \Delta C_s \tag{48}$$

where J_s, D_s, and C_s are the mass flux, diffusivity, and concentration of the solute, respectively, within the membrane. The phenomenological solute transport coefficient can be defined as

$$B = \frac{D_s}{\delta_m} \tag{49}$$

which is called the solute permeability. It is often assumed that D_s is independent of the solute concentration, but maybe varies with temperature. In Eq. (48),

ΔC_s indicates the transmembrane concentration difference, measured on the exterior surfaces of the membrane with empirically measured B.

2.3.2. Solvent and solute fluxes

The solvent flux J_w is proportional to the effective pressure, of which the osmotic pressure difference can be more accurately represented as:

$$\Delta\pi = \pi_m - \pi_p \tag{50}$$

The van't Hoff equation indicates that the (absolute) osmotic pressure is linearly proportional to the solute concentration, unless the concentration is very high near the solubility limit. In this case, the solution-diffusion model is equivalent to the osmotic pressure model and then we can have:

$$\Delta\pi = \pi_f\left(\frac{C_m}{C_f} - \frac{C_p}{C_f}\right) \tag{51}$$

and hence using Eq. (32) we make a relationship between the thermodynamic variable $\Delta\pi$ and the hydrodynamic variable J_w through the mass transfer coefficient k.

$$\Delta\pi = \pi_f R_{\text{obs}} e^{J_w/k_f} \tag{52}$$

By substituting Eq. (52) in (44), we obtain

$$J_w = A\left(\Delta P - \pi_f R_{\text{obs}} e^{J_w/k_f}\right) \tag{53}$$

which needs to be solved iteratively for J_w with an estimated value of k_f. Phenomenologically, the permeate flux increases if the applied pressure increases. The enhanced permeate flux contributes additionally to the convective solute transport toward the membrane surface, which brings more solutes to the membrane and hence increases C_m. The osmotic pressure on the membrane surface π_m therefore increases exponentially with J_w (See Eq. (52) depending on the ration of J_w/k_f). As a consequence, the net pressure, the driving force of the solute permeation, does not increase as much as ΔP increases. This is because the concentration polarization causes the reduction of the driving force as indicated in Eq. (52). Since J_w is on both sides of Eq. (53), a nonlinear or iterative solver is required to calculate J_w. If the mass transfer coefficient is larger than the permeate flux or

$$\frac{J_w}{k_f} < 1 \quad \text{and} \quad \left(\frac{J_w}{k_f}\right)^2 \ll 1$$

then we can expand the exponential term in Eq. (52) as

$$e^{J_w/k_f} \simeq 1 + \frac{J_w}{k_f} + O\left(\frac{J_w^2}{k_f^2}\right) \tag{54}$$

In this case, we derive an analytic expression for the permeate flux:

$$J_w = A_{\text{eff}}\left(\Delta P - \pi_f R_{\text{obs}}\right) \tag{55}$$

under the influence of the C_p, where the effective solvent permeability A_{eff} is calculated as

$$A_{\text{eff}} = \frac{A}{1 + A\pi_f R_{\text{obs}} k_f^{-1}} \tag{56}$$

Eq. (55) explains the solvent permeation giving a different picture from that of Eq. (53). $\pi_f R_{\text{obs}}$ indicates the osmotic pressure difference between the feed and permeate streams. The effective solvent permeability A_{eff}, which is smaller than A, includes the resistance for solvent permeation from the membrane as well as the CP layer. When the concentration polarization is negligible and so its thickness is very small, i.e., $\delta_p \to 0$, then the mass transfer coefficient k_f diverges, because a finite concentration difference exists within a CP layer of zero thickness $k_f^{-1} \to 0$. The effective sol

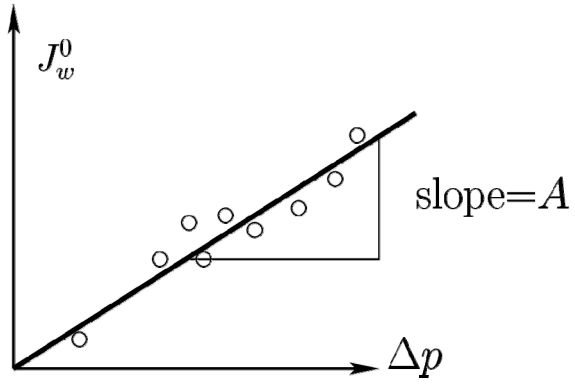

Fig. 5. Schematic of the pure water flux with respect to the applied pressure.

vent permeability A_{eff} converges to A as the CP layer disappears.

In the solution-diffusion model, the driving force for the solute flux is the concentration difference between the membrane surface and the permeate stream. Replacing ΔC_s in Eq. (48) by $C_m - C_p$ gives

$$J_s = B\left(C_m - C_p\right) \tag{57}$$

Again, note that B has the same unit of J_w [m/s]. We rewrite Eq. (57), using Eq. (29), as

$$J_s = BC_f R_{\text{obs}} e^{J_w/k_f} \tag{58}$$

which implies that J_s increases exponentially with respect to J_w. Note that the solute flux must be equal to the permeate concentration multiplied by the permeate flux:

$$J_s = C_p J_w = C_f(1 - R_{\text{obs}})J_w \tag{59}$$

Rigorously, J_s in Eq. (58) indicates the solute flux through the membrane interior driven by the external concentration difference, $C_m - C_p$. Eq. (59) is based on the global mass balance implying that the solute molecules are uniformly mixed in the permeate stream after they have passed through the membrane.

2.3.3. Parameter estimation

2.3.3.1. Solvent permeability

The solvent permeability A is an intrinsic material constant of a specific membrane and so needs to be experimentally measured. When the feed stream of zero concentration ($C_f = 0$) is filtered using an RO membrane, we have

$$A = \frac{J_w^0}{\Delta P} \tag{60}$$

where J_w^0 indicates the permeate flux of zero feed concentration. Using pure water, a series of filtration experiments can be conducted to measure J_w^0 with respect to ΔP as schematically shown in Fig. 5. The slope of the flux vs. pressure line can be calculated using a simple linear regression method, which is the value of the most probable A.

2.3.3.2. Solute permeability

Let us simply assume that B is also a constant within typical ranges of the solute concentration and applied pressure in normal RO processes. From Eqs. (53), (58) and (59), we obtain:

$$R_{\text{obs}} e^{J_w/k_f} = \frac{A\Delta P - J_w}{A\pi_f} = \frac{(1 - R_{\text{obs}})J_w}{B} \tag{61}$$

which leads to

$$\frac{B}{A} = \frac{\pi_p J_w}{J_w^0 - J_w} \tag{62}$$

where $\pi_p = \pi_f\,(1 - R_{\text{obs}})$ is the osmotic pressure of the permeate stream and $J_w^0 - J_w$ indicates the permeate flux lost from the pure water flux J_w^0 due to the concentration polarization.

2.3.3.3. Low flux limit

When the permeate flux is low due to small effective pressure, the following approximations can be

Table 1. Exponents of the Mass Transfer Coefficients in terms of Channel Geometry and Flow Regions

flow	geometry	*a*	*b*	*c*	*d*
laminar	tube	1.62	1/3	1/3	1/3
laminar	rectangular	1.85	1/3	1/3	1/3
turbulent	tube	0.44	3/4	1/3	0
turbulent	rectangular	0.44	3/4	1/3	0

made. The intrinsic rejection R_{int} converges to the observed rejection, $R_{\mathrm{int}} \to R_{\mathrm{obs}}$, because the CP must be negligible on the membrane surface, i.e., $C_m \to C_f$, and hence $\pi_m \to \pi_f$. The solute flux is than

$$J_s = C_p J_w = B_0 \left(C_f - C_p\right) \tag{63}$$

which gives

$$B_0 = J_w \frac{1 - R_{\mathrm{obs}}}{R_{\mathrm{obs}}} \tag{64}$$

where the subscript $\mathbf{0}$ indicates no or negligible concentration polarization. Then, B of Eq. (61) can be expressed as:

$$B = B_0 e^{-J_w/k_f} \tag{65}$$

If $J_w/k_f \ll 1$, then B converges to B_0 of the dilute limit

2.3.3.4. Mass transfer coefficient

In system design and performance evaluation of RO processes, estimation of the mass transfer coefficient k_f is of great importance. A number of experiments can be conducted and accumulated data can be used to create empirical correlations for later use. Here, k_f can be represented using the solvent flux Eq. (53) and the solute flux Eq. (58), which are

$$\frac{1}{k_f} = \frac{1}{J_w} \ln \frac{J_w^0 - J_w}{A \pi_f R_{\mathrm{obs}}} \tag{66}$$

and

$$\frac{1}{k_f} = \frac{1}{J_w} \ln \frac{(1 - R_{\mathrm{obs}}) J_w}{B R_{\mathrm{obs}}} \tag{67}$$

respectively. Values of k_f estimated using the above two equations should be comparable within a tolerable error.

2.3.4. Empirical correlations

When a feed solution is physico-chemically characterized and a module geometry is given, the crossflow speed u is almost the only controllable parameter to change the mass transfer coefficient k_f. For dimensionless analysis, Sherwood number is often represented as a function of Reynolds and Schmidt numbers and the aspect ratio of the channel geometry. (See section A.2 for details.) Table 1 shows exponent values of a, b, c, and d in Eq. (A.9). For laminar flow, a of a rectangular channel is slightly higher than that of a cylindrical tube, and all other exponents are equally $1/3$. Influences of Re, Sc, and module geometry on the k_f must be similar in cylindrical and rectangular channels while a represents the effect of the cross-section shape. For turbulent flow, a, b, and c are same for the cylindrical and rectangular channels and interestingly $d = 0$. Due to the complex nature of the turbulent flow field, the effect of hydraulic diameter vanishes. This must be bacause the wetted surface area in the turbulence fails to provide a controllable impact on the mass transfer.

2.3.5. Long membrane modules

Fig. 6 shows a schematic of crossflow RO filtration. For a short membrane, the retentate concentration is

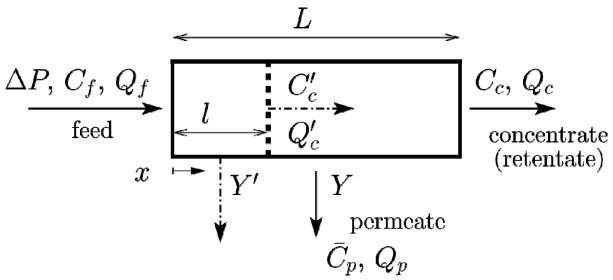

Fig. 6. RO schematic with local balance.

$$C_c = \frac{C_f - C_p Y}{1 - Y} \tag{68}$$

which implicitly neglects the concentration variation in the longitudinal direction, as shown in Fig. 2. For a long membrane, Eq. (68) holds its validity only if C_p is replaced by its length-averaged value:

$$\bar{C}_p = \frac{1}{L}\int_0^L C_p(x)\mathrm{d}x \tag{69}$$

where $C_p(x)$ is a local permeate concentration at $x\,(0 < x < L)$. A local average concentration of $C_p(x)$ is denoted as

$$\bar{C}'_p = \frac{1}{x}\int_0^x C_p(x')\mathrm{d}x' \tag{70}$$

Then, the retentate concentration of Eq. (68) can be re-written as

$$C_c = \frac{C_f - \bar{C}_p Y}{1 - Y} \tag{71}$$

where Y is the (global) recovery ratio defined in Eg. (2).

2.3.5.1. Mean osmotic pressure in the bulk phase

To apply the solution-diffusion model for a long membrane module, a longitudinally mean osmotic pressure $\bar{\pi}$ is necessary to calculate the mean transmembrane osmotic pressure: $\Delta\pi = \bar{\pi} - \pi_p$. A good approximation, especially for membrane array design, can be

$$\bar{\pi} = \frac{\pi_f + \pi_c}{2} \tag{72}$$

where $\pi_c = \pi(C_c)$. Note that Eq. (72) does not include the effect of the concentration polarization phenomena in the transverse direction. This forceful decoupling of mass balance equations in the transverse and longitudinal direction allows concise analytical solutions, which are later combined using empirical correlations. The mass transfer coefficient k_f, estimated using an empirical correlation, implicitly includes effects of the membrane length and the channel cross-section in addition to the transport mechanisms.

2.3.5.2. Mulder's theory

Now we apply the same analysis at $x = L$. For a partial membrane of length x from 0, C_c and C_p of a full membrane are replaced by their partial values C'_c and C'_p, respectively:

$$C'_c = \frac{C_f - C'_p Y'}{1 - Y'} \tag{73}$$

where Y' is a local recovery ratio for the partial membrane of length x. To solve this, we need an additional relationship such as

$$\frac{C'_p}{1 - R} = \langle C'_c \rangle \tag{74}$$

for which Mulder[34] assumed that

$$< C'_c >= \frac{1}{Y'}\int_0^{Y'} C'_c(Y)\mathrm{d}Y \tag{75}$$

Substitution of Eq. (73) and (75) in (74) gives

$$C'_c \cdot (1 - Y') = C_f - (1 - R)\int_0^{Y'} C'_c\,\mathrm{d}Y \tag{76}$$

which is an integral equation for C_c'. We differentiate Eq. (76) with respect to Y' to have

$$\frac{\mathrm{d}C_c'}{C_c'} = R\frac{\mathrm{d}Y'}{1-Y'} \tag{77}$$

and integrate it such that

$$\int_{C_f}^{C_c}\frac{\mathrm{d}C_c'}{C_c'} = R\int_0^Y \frac{\mathrm{d}Y'}{1-Y'} \tag{78}$$

to obtain

$$C_c = C_f\cdot(1-Y)^{-R} \tag{79}$$

Substitution of (79) in (71) gives the mean permeate concentration:

$$\bar{C_p} = C_f\frac{1-(1-Y)^{1-R}}{Y} \tag{80}$$

represented as a function of C_f, R, and Y. In this approach, Y implicitly includes impacts of A, A_m and ΔP, and R contains the rejecting role of B.

Examples in section A.3 indicate that Mulder's theory is valid when the rejection ratio is high, such as standard RO processes. The key Eqs. (79) and (80) stem from the partial mass balance Eqs. (74) and (75). The solution-diffusion model uses specific permeability values of A and B to iteratively calculate the permeate concentration. As the CP is incorporated into the solution-diffusion model, C_m is considered higher than C_f, but does not explicitly include variation of C_p in the longitudinal direction (from the inlet to the exit of the membrane module). An empirical correlation for the mass transfer coefficient k_f implicitly includes the length-averaged dimensionless numbers, and perhaps so does C_m. Therefore, combination of the solution-diffusion model and k_f, estimated using an empirical correlation, is conceptually equivalent to Mulder's intuitive assumption:

$$\frac{\bar{C_p'}}{1-R} = \frac{1}{Y'}\int_0^{Y'} C_c'(Y)\mathrm{d}Y$$

Usually, vendors provide a rejection ratio for a membrane, measured at a reference condition, which, in this case, can be used as an intrinsic constant similar to A or B. Mulder's theory allows us to practically estimate the product permeate concentration using R and Y without dealing with specific transport models.

In section 2.1, a membrane is characterized using ten variables. Of these, six variables of A, B, A_m, ΔP, C_f and Q_f are known. The four remaining ones are calculated using the same number of equations, which are global mass balances of Eqs. (3) and (4), and solvent and solute fluxes of Eqs. (5) and (6), respectively. In Mulder's approach, the membrane is treated as a black box of known R and Y so that the variable set includes eight elements $\{R, Y, C_f, Q_f, C_p, Q_p, C_c, Q_c\}$. When R, Y, C_f, and Q_f are known, then definitions of R and Y, and global mass balance equations of solutes and solvent will be used to calculate the same total number of unknowns, such as $\{C_p, Q_p, C_c, Q_c\}$.

2.4. Coupled Governing Equations

An accurate governing equation without the artificial decoupling between the transverse and longitudinal directions is

$$\frac{\partial C}{\partial t} = \frac{\partial}{\partial y}\left(D\frac{\partial C}{\partial y}\right) - u(y)\frac{\partial C}{\partial x} - v_w(x)\frac{\partial C}{\partial y} \tag{81}$$

where the solute diffusivity D is often assumed to be constant and the longitudinal diffusion is discarded by assuming $\partial^2 C/\partial x^2 \ll \partial^2 C/\partial y^2$. Within the CP layer, the crossflow velocity is often represented as a linear shear flow with respect to y:

$$u(y) = \gamma y \tag{82}$$

where

$$\gamma = \left[\frac{\partial u}{\partial y}\right]_{y=0} \tag{83}$$

is a shear rate on the membrane surface. The mathematical rigor of the coupled governing equation is closely related to the exponential dependence of the concentration near membrane surface on the permeate flux (see Eq. (27))[35,36]. Only a numerical solution seemed to be available for the 2D convection and diffusion of solutes on the membrane surface. A general solution of Eq. (81) was developed using Airy functions, but coefficients were obtained by numerical integrations[37]. This work discovered that an inflection point of the concentration profile exists in the longitudinal crossflow direction. But, even if these analytic approaches provide a fundamental insight of crossflow membrane filtration, they are still restricted to solute migration on the flat, slip-less surface providing the linear shear field of Eq. (82). It is formidably difficult to develop an analytic solution of the 2D governing equation if one or some of the followings are additionally considered: the presence of spacers, transient hydraulic pressure for pulsing, curved channels, and parabolic or nonlinear flow fields.

2.5. Fouling indexes and scaling potential

2.5.1. Modified fouling index (MFI) for colloidal fouling

When colloidal particles deposit on the membrane surface (typically, but not limited to, MF or UF membranes), the resistance-in-series model represents the permeate flux:

$$J_w = \frac{\Delta P}{\eta\,(R_m + R_c)} \tag{84}$$

where R_c is the resistance of the cake layer, i.e., temporarily or permanently built deposit layer of solid materials such as nano- or colloidal particles, (deformable) macromolecules, and combined forms. In the dead-end filtration or at the initial stage of the crossflow filtration, R_c continuously increases with respect to time, and moreover, often causes noticeable declining trends of the permeate flux. The specific cake resistance is defined as

$$r_c = R_c/\delta_c \tag{85}$$

which is independent on the cake thickness δ_c unless the cake layer has a heterogeneous mass density. In principle, the specific resistance is an inverse of the hydraulic permeability κ, i.e., $r_c = \kappa^{-1}$, which is generally a function of particle size, particle shape, and cake porosity. If particulate materials are perfectly removed by a membrane, the amount of particle mass transported from the bulk (feed) phase to the membrane surface is equal to the particle mass accumulated on the membrane surface, which is mathematically written as

$$\phi_f V = \phi_c A_m \delta_c \tag{86}$$

where ϕ_f and ϕ_c are particle volume fractions in the feed solution and of the cake layer, respectively, and V is the permeate volume, i.e., the solvent volume passed through the membrane having the surface area A_m. Substitution of (86) in (85) gives

$$R_c = \alpha V \tag{87}$$

where $\alpha = \phi_f r_c/\phi_c A_m$ is the proportionality between the cake resistance and the permeate volume. Eq. (87) indicates that the cake resistance increases as water is filtered by the membrane. By definition, the permeate flux is written as

$$J_w = \frac{1}{A_m}\frac{\mathrm{d}V}{\mathrm{d}t} \tag{88}$$

as it is proportional to the volume of produced solvent per unit time, i.e., dV/dt. Substitution of (87) and (88) in (84) provides

$$\frac{1}{A_m}\frac{\mathrm{d}V}{\mathrm{d}t} = \frac{\Delta P}{\eta\,(R_m + \alpha V)} \tag{89}$$

which is simply the first order ordinary differential equation of the filtered volume V, rewritten as

$$\eta\,(R_m + \alpha V)\mathrm{d}V = \Delta P \mathrm{d}t A_m \tag{90}$$

in an integrable form. Integration of this equation using the initial condition of $V(t=0)=0$ gives

$$\frac{t}{V} = C_1 + C_2 V \tag{91}$$

where

$$C_1 = \frac{\eta R_m}{A_m \Delta P} \tag{92}$$

is the y-intercept of t/V versus V plot and

$$C_2 = \frac{\eta \phi_f r_c}{2\phi_c A_m^2 \Delta P} \equiv \mathrm{MFI} \tag{93}$$

is the slope, which is defined as modified fouling index (MFI)[38,39]. This MFI cannot be easily calculated using Eq. (93), because the cake volume fraction ϕ_c is neither known nor (easily) measurable and r_c is a complex non-linear function of ϕ_c. Theoretical calculation of MFI is additionally challenging, if ϕ_c strongly depends on inter-particle and particle-membrane interactions.

2.5.2. Combined fouling index (CFI)

When the feed solution contains both salt ions of high concentration and colloidal particles, the permeate flux may be expressed as a combination of the osmotic pressure model and the resistance-in-series model:

$$J_w = \frac{\Delta P - \Delta\pi_m}{\eta\,(R_m + R_c)} \tag{94}$$

where $\Delta\pi_m\,(=\pi_m - \pi_f)$ is the transmembrane osmotic pressure difference in the presence of CP. Consider that the cake layer exists inside the CP layer of salt ions, i.e., $\delta_p > \delta_c$, where δ_p is the thickness of the CP layer. Then, we define

$$\delta_s = \delta_p - \delta_c \tag{95}$$

which is the partial thickness of the concentration polarization layer above the cake layer, within which the tangential cross flow velocity is assumed to be negligible. The surface of the cake layer may provide the no-slip boundary condition, which is similar to the (bare) membrane surface without the particle deposition. Then, the mass balance Eq. (24) can be employed using the solute diffusivity changing with respect to y:

$$D = \begin{cases} D_0 & \text{for} \quad \delta_c < y < \delta_p \\ D_0 \dfrac{\epsilon}{\tau} & \text{for} \quad 0 < y < \delta_c \end{cases} \tag{96}$$

where $\epsilon\,(=1-\phi_c)$ is the cake porosity and τ is the diffusive tortuosity. In Eq. (24), $\mathrm{d}y/(C-C_p)$ is multiplied on both sides to give

$$\int_{C_m}^{C_f} \frac{\mathrm{d}C}{C - C_p} = -\int_0^{\delta_c} \frac{J_w \tau}{D_0 \varepsilon} dy - \int_{\delta_c}^{\delta_p - \delta_c} \frac{J_w}{D_0} dy \tag{97}$$

which is solved as

$$\ln \frac{C_f - C_p}{C_m - C_p} = -\frac{J_w}{D_0}\left(\frac{\tau}{\epsilon}\delta_c + \delta_s\right) \tag{98}$$

The cake volume fraction ϕ_c is often assumed to be a random close packing ratio of 0.64[40,41], and the diffusive tortuosity τ is in principle greater than 1.0, varying with ϕ_c and the internal structure of the cake layer. For a thick cake layer, the concentration polarization above the cake layer does not significantly contribute to the permeate flux in magnitude. So, one can approximate Eq. (98) by removing δ_s as

$$\frac{C_m - C_p}{C_f - C_p} = \exp\left(\frac{J_w \delta_c}{D_0 \epsilon/\tau}\right) = e^j \tag{99}$$

where we define a dimensionless permeate flux

$$j = \frac{J_w}{k_c} \tag{100}$$

and

$$k_c = \frac{D_0}{\delta_c \tau/\epsilon} \tag{101}$$

interpreted as the diffusive mass-transfer coefficient of solute ions in the cake layer of porosity ε. The denominator of Eq. (101), $\delta_c \tau/\epsilon$, can be considered as the effective path length of diffusing solutes within the cake layer, which is longer than that in the void space.

Substitution of Eq. (99) in (94) gives the final equation to solve for j:

$$j = \frac{\Delta P - \pi_f R_{\text{obs}} e^j}{k_c \eta (R_m + R_c)} \tag{102}$$

Similar to the previous case, we assume $j < 1$ to use

$$e^j = 1 + j + O(j^2) \tag{103}$$

and substitute Eq. (103) in (102). We then replace j by $(k_c A_m)^{-1} \mathrm{d}V/\mathrm{d}t$ and use Eq. (87) to give

$$\eta\left[R_m + \frac{\pi_f R_{\text{obs}}}{k_c \eta} + \alpha V\right]\mathrm{d}V = (\Delta P - \pi_f R_{\text{obs}}) A_m \mathrm{d}t \tag{104}$$

Integration of both sides using an initial condition of $V = 0$ at $t = 0$ provides

$$t = \left(\frac{\eta R_m}{A_m \mathrm{d}P}\right)\left(\frac{1 + \hat{\pi}_f \frac{J_{w0}}{k_c}}{1 - \hat{\pi}_f}\right) V + \left(\frac{\eta \phi_f r_c}{2\phi_c A_m^2 \Delta P}\right)\frac{1}{(1 - \hat{\pi}_f)} V^2$$

which is simplified to

$$\frac{t}{V} = C_1\left(\frac{1 + \hat{\pi}_f \frac{J_{w0}}{k_c}}{1 - \hat{\pi}_f}\right) + \frac{\text{MFI}}{(1 - \hat{\pi}_f)} V \tag{105}$$

where

$$\hat{\pi}_f = \frac{\pi_f R_{\text{obs}}}{\Delta P} \tag{106}$$

indicates the ratio of the osmotic pressure of the net concentration $\pi_f R_{obs}$ to the applied pressure ΔP. Now, we can take the proportional constant of V in Eq. (105) to define the combined fouling index (CFI) as

$$\text{CFI} = \frac{\text{MFI}}{1 - \hat{\pi}_f} \tag{107}$$

The absence of the salt ions in the feed stream can be considered by setting $\hat{\pi}_f = 0$, which makes CFI converge to MFI and equivalertly Eq. (105) equal to (91). In this case, applications are limited to MF or UF processes. The fouling tendency of RO desalination can be quantified using the CP factor β, defined as

$$\beta = C_m/C_f \tag{108}$$

which can be estimated using the measured permeate flux J_w and the empirically-determined mass transfer coefficient k_f in Eq. (27). In addition to β, CFI can be used to estimate the combined fouling tendency in the presence of both ionic and particulate species. Note that CFI is always larger than MFI. For example, if ΔP is set as twice seawater osmotic pressure π_{sw}, then we calculate $\hat{\pi}_f = 2\pi_{\text{sw}}/\pi_{\text{sw}} = 2$ and CFI = 2 × MFI using Eq. (107). Related experimental and modeling studies can be found elsewhere[42-45].

3. Concluding Remarks

In this study, I briefly reviewed the fundamentals of reverse osmosis processes, based on the solution-diffusion model. Specific variations of output variables such as concentrations and outflow rates of the permeate and brine streams are characterized with respect to the input and operating parameters. Transverse variations of the solute concentration are reviewed by solving the decoupled convection-diffusion equation. Mulder's theory is discussed to explain the longitudinal variations of permeate flux, which primarily controls the rejection and recovery ratios. The solution-diffusion model was also reviewed using principles and concepts of statistical mechanics. Finally, the degree of combined fouling (by both ionic solutes and particulate materials) is quantified using a novel combined fouling index (CFI) as an extension of the modified fouling index (MFI).

In environmental engineering, which is the discipline closest to mother nature, a holistic understanding of transport phenomena at the basic level of thermodynamics, statistical mechanics, and fluid mechanics is as important as practically dealing with designing, optimizing, and maintaining specific processes. Hopefully, my incomplete manuscript can be a stepping stone for future membrane engineers, who may resolve the impending global water shortage.

Appendix

A.1. Proof of Eq. (27)

The permeate flux J_w, the permeate concentration C_p, and the solute diffusivity D are assumed to be constant. Eq. (24) is rewritten, using the net or excessive concentration $C' = C - C_p$, as

$$D\frac{\mathrm{d}C'}{\mathrm{d}y} = -J_w C' \tag{A.1}$$

Because only C' is a sole function of y, one rewrites Eq. (A.1) as

$$\frac{\mathrm{d}C'}{C'} = -\frac{J_w}{D}\mathrm{d}y \tag{A.2}$$

Integration of Eq. (A.2) gives

$$\ln C' = -\frac{J_w}{D}y + \text{constant} \tag{A.3}$$

of which the constant is determined using the boundary condition of Eq. (25):

$$\ln\left[C_m - C_p\right] = \text{constant} \tag{A.4}$$

The boundary condition of Eq. (26) on the top of the CP layer provides

$$\ln\left[C_f - C_p\right] = -\frac{J_w}{D}\delta_p + \text{constant} \tag{A.5}$$

Substitution of Eq. (A.4) in (A.5) generates

$$\frac{C_m - C_p}{C_f - C_p} = \exp\left[+\frac{J_w}{D/\delta_p}\right] \tag{A.6}$$

in which the solute diffusivity per CP layer thickness, D/δ_m, refers to the mass transfer coefficient k_f of the same dimension of the permeate flux J_w. Substitution of Eq. (A.4) in (A.3) gives the solute concentration $C(y)$ as a function of the distance from the membrane surface y:

$$\frac{C(y) - C_p}{C_m - C_p} = \exp\left[-\frac{J_w y}{D}\right] \quad \text{for} \quad 0 < y < \delta_p \tag{A.7}$$

The concentration exponentially increases from C_f at the CP layer boundary to C_m on the membrane surface.

A.2. Dimensionless number analysis

The performance of a membrane is typically estimated using the recovery and rejection ratios, which

are primarily determined by A and B, respectively, These are intrinsic material properties of the membrane. On the other hand, the mass transfer coefficient k_f is strongly dependent on fluid dynamics and module geometry. In engineering and applied sciences, dimensionless numbers are often used to represent correlations between representative physical quantities. The Sherwood number (Sh) includes the mass transfer coefficient such as

$$\mathrm{Sh} = \frac{k_f d_h}{D} = \frac{\text{convective mass transfe rate}}{\text{diffusive mass transfer rate}} \quad \text{(A.8)}$$

implying the significance of the convection over the diffusion of solutes, where d_h is the hydraulic diameter. The Sherwood number is often represented as a function of Reynolds (Re) and Schmidt (Sc) numbers:

$$\mathrm{Sh} = a\,\mathrm{Re}^b\,\mathrm{Sc}^c\left(\frac{d_h}{L}\right)^d \quad \text{(A.9)}$$

where L is the membrane (or channel) length, and $a-d$ are constants. Here, d_h/L can be considered as the aspect ratio of the flow channel. The Reynolds number measures a ratio of inertial to viscous forces for given flow conditions, which is often defined as

$$\mathrm{Re} = \frac{u d_h}{\nu} = \frac{u \rho d_h}{\eta} \quad \text{(A.10)}$$

where u is the cross flow speed, ρ is the fluid density, and η and ν are the absolute and kinematic viscosities, respectively. In the case of flow through a straight pipe with a circular cross-section, fluid motion will be laminar at $\mathrm{Re} < 2000$, whereas at $\mathrm{Re} > 4000$, the flow is turbulent. Finally, the Schmidt number represents a ratio of momentum to mass diffusivity:

$$\mathrm{Sc} = \frac{\nu}{D} \quad \text{(A.11)}$$

A.3. Application of Mulder's theory to Seawater Desalination

For example, an RO desalination process has a feed water of 35,000 ppm and the rejection ratio of the selected membrane is reported by a vendor as 99.00%. If the process is operated for 60% recovery, then the permeate concentration is predicted as

$$\bar{C_p} = C_f \frac{1-(1-0.6)^{1-0.99}}{0.6} = C_f \times 0.01520 = 532.06\ \text{ppm} \quad \text{(A.12)}$$

If so, one calculates

$$1 - \frac{\bar{C_p}}{C_f} = 0.9848 \quad \text{(A.13)}$$

which is close enough to the given rejection of 0.9900. If we replace the rejection by 40% (such as that of nanofiltration), then we calculate

$$\bar{C_p} = C_f \frac{1-(1-0.6)^{1-0.40}}{0.6} = C_f \times 0.7048 = 24670.33\ \text{ppm} \quad \text{(A.14)}$$

and

$$1 - \frac{\bar{C_p}}{C_f} = 0.2951 \quad \text{(A.15)}$$

which is erroneously different from the original value of 40%.

Reference

1. S. Loeb and S. Sourirajan, "Sea water demineralization by means of semipermeable membrane", *UCLA report*, **60-60**, 1 (1960).

2. D. Talbot, "Megascale Desalination", MIT Technology Review, March/April (2015).
3. S. Loeb, "The Loeb-Sourirajan Membrane: How It Came About", in "Synthetic Membranes", *Am. Chem. Soc*., **153**, 1 (1981).
4. J. Glater, "The early history of reverse osmosis membrane development", *Desalination*, **117**, 297 (1998).
5. S. Sourirajan, "Reverse Osmosis", Academic Press, Los Angeles, CA (1970).
6. C. E. Reid and E. J. Breton, "Water and ion flow across cellulosic membranes", *J. Appl. Polymer Sci.*, **1**, 133 (1959).
7. T. A. Orofino, H. B. Hopfenberg, and V. Stannett, "Characterization of penetrant clustering in polymers", *J. Macromol. Sci. B*, **3**, 777 (1969).
8. H. K. Lonsdale, U. Merten, and R. L. Riley, "Transport properties of cellulose acetate osmotic membrane", *J. Appl. Polymer Sci.*, **9**, 1341 (1965).
9. R. L. Riley, H. K. Lonsdale, C. R. Lyons, and U. Merten, "Preparation of ultrathin reverse osmosis membranes and the attainment of theoretical salt rejection", *J. Appl. Polymer Sci.*, **11**, 2143 (1967).
10. T. K. Sherwood, P. L. T. Brian, and R. E. Fisher, "Desalination by reverse osmosis process", *I&EC Fund.*, **17**, 2 (1968).
11. J. P. Agrawal and S. Sourirajan, "Specification, selectivity, and performance of porous cellulose acetate membranes in reverse osmosis", *I&EC Proc. Des. Devel*., **8**, 439 (1969).
12. E. Glueckauf, "The distribution of electrolytes between cellulose acetate membranes and aqueous solutions", *Desal.*, **18**, 155 (1976).
13. J. Wijmans and R. Baker, "The solution-diffusion model: A review", *J. Membr. Sci*., **107**, 1 (1995).
14. D. R. Paul, "Reformulation of the solution-diffusion theory of reverse osmosis", *J. Membr. Sci*., **241**, 371 (2004).
15. L. Onsager, "Reciprocal relations in irreversible processes. I.", *Phys. Rev.*, **37**, 405 (1931).
16. L. Onsager, "Reciprocal relations in irreversible processes. II", *Phys. Rev.*, **38**, 2265 (1931).
17. O. Kedem and A. Katchalsky, "Thermodynamic analysis of the permeability of biological membranes to non-electrolytes", *Biochim. Biophys. Acta*, **27**, 229 (1958).
18. K. S. Spiegler and O. Kedem, "Thermodynamics of hyperfiltration (reverse osmosis): criteria for efficient membranes", *Desal*., **1**, 311 (1966).
19. M. Soltanieh and W. N. Gill, "Review of reverse osmosis membranes and transport models", *Chem. Eng. Comm.*, **12**, 279 (1981).
20. D. Potts, R. Ahlert, and S. Wang, "A critical review of fouling of reverse osmosis membranes", *Desal.*, **36**, 235 (1981).
21. M. F. A. Goosen, S. S. Sablani, H. Al-Hinai, S. Al-Obeidani, R. Al-Belushi, and D. Jackson, "Fouling of reverse osmosis and ultrafiltration membranes: A critical review", *Sep. Sci. Tech.* **39**, 2261 (2005).
22. D. Li and H. Wang, "Recent developments in reverse osmosis desalination membranes", *J. Mat. Chem.*, **20**, 4551 (2010).
23. S. Sobana and R. C. Panda, "Identification, modelling, and control of continuous reverse osmosis desalination system: A review", *Sep. Sci. Tech.*, **46**, 551 (2011).
24. K. P. Lee, T. C. Arnot, and D. Mattia, "A review of reverse osmosis membrane materials for desalination-Development to date and future potential", *J. Membr. Sci.*, **370**, 1 (2011).
25. L. Malaeb and G. M. Ayoub, "Reverse osmosis technology for water treatment: State of the art review", *Desal*., **267**, 1 (2011).
26. S. Sablani, M. Goosen, R. Al-Belushi, and M. Wilf, "Concentration polarization in ultrafiltration and reverse osmosis: A critical review", *Desal.*, **141**, 269 (2001).
27. G. Amy, N. Ghaffour, Z. Li, L. Francis, R. V. Linares, T. Missimer, and S. Lattemann, "Membrane-based seawater desalination: Present and future prospects", *Desal.*, **401**, 16-21 (2017).
28. M. A. Shannon, P. W. Bohn, M. Elimelech, J. G. Georgiadis, B. J. Mariñas, and A. M. Mayes,

"Science and technology for water purification in the coming decades", *Nature*, **452**, 301 (2008).
29. M. Elimelech and W. A. Phillip, "The future of seawater desalination: energy, technology, and the environment.", *Science*, **333**, 712 (2011).
30. B. E. Logan and M. Elimelech, "Membrane-based processes for sustainable power generation using water", *Nature*, **488**, 313-319 (2012).
31. H. B. Park, J. Kamcev, L. M. Robeson, M. Elimelech, and B. D. Freeman, "Maximizing the right stuff: The trade-off between membrane permeability and selectivity.", *Science*, **356**, 1 (2017).
32. W. J. Koros and C. Zhang, "Materials for next-generation molecularly selective synthetic membranes", *Nat. Mat.*, **16**, 289 (2017).
33. H. K. Lonsdale, U. Merten, and R. L. Riley, "Transport properties of cellulose acetate osmotic membranes", *J. Appl. Polymer Sci.*, **9**, 1341 (1965).
34. M. Mulder, Basic Principles of Membrane Technology, Kluwer Academic Publishers, Boston, MA (1996).
35. A. L. Zydney and C. K. Colton, "A concentration polarization model for the filtrate flux in cross-flow microfiltration of particulate suspensions", *Chem. Eng. Comm.*, **47**, 1 (1986).
36. A. Zydney, "Stagnant film model for concentration polarization in membrane systems", *J. Membr. Sci.*, **130**, 275 (1997).
37. A. S. Kim, "Permeate flux inflection due to concentration polarization in crossflow membrane filtration: A novel analytic approach", *Euro. Phys. J. E*, **24**, 331 (2008).
38. J. C. Schippers and J. Verdouw, "The modified fouling index, a method of determining the fouling characteristics of water", *Desal.*, **32**, 137 (1980).
39. S. Khirani, R. Ben Aim, and M. H. Manero, "Improving the measurement of the Modified Fouling Index using nanofiltration membranes (NF-MFI)", *Desal.*, **191**, 1 (2006).
40. G. Mason, "Radial Distribution of the random close packing of equal spheres", *Nature*, **217**, 733 (1968).
41. W. M. Visscher and M. Bolsterli, "Random packing of equal and unequal spheres in two and three dimensions", *Nature*, **239**, 504 (1972).
42. A. E. Contreras, A. S. Kim, and Q. Li, "Combined fouling of nanofiltration membranes: Mechanisms and effect of organic matter", *J. Membr. Sci.*, **327**, 87 (2009).
43. A. S. Kim, A. E. Contreras, Q. Li, and R. Yuan, "Fundamental mechanism of three-component combined fouling with experimental verification", *Langmuir*, **25**, 7815 (2009).
44. Y. Yu, S. Lee, K. Hong, and S. Hong, "Evaluation of membrane fouling potential by multiple membrane array system (MMAS): Measurements and applications", *J. Membr. Sci.*, **362**, 279 (2010).
45. Y. Kim, M. Elimelech, H. K. Shon, and S. Hong, "Combined organic and colloidal fouling in forward osmosis: Fouling reversibility and the role of applied pressure", *J. Membr. Sci.*, **460**, 206 (2014).